European Journal of Applied Mathematics (2025), **36**, pp. 811–828
doi:10.1017/S095679252400069X

CAMBRIDGE UNIVERSITY PRESS

PAPER

A diffusive plant-sulphide model: spatio-temporal dynamics contrast between discrete and distributed delay

Yonghui Xia[1], Jianglong Xiao[2] and Jianshe Yu[3]

[1]School of Mathematics, Foshan University, Foshan, China
[2]School of Mathematical Sciences, Zhejiang Normal University, Jinhua, China
[3]College of Mathematics and Information Sciences, Guangzhou University, Guangzhou, China
Corresponding author: Jianshe Yu; Email: jsyu@gzhu.edu.cn

Received: 07 March 2024; **Revised:** 12 July 2024; **Accepted:** 16 July 2024; **First published online:** 28 October 2024

Keywords: diffusion; Hopf bifurcation; delay; stability

2020 Mathematics Subject Classification: 34K18 (Primary); 34C23, 35B32 (Secondary)

Abstract

This paper studies the spatio-temporal dynamics of a diffusive plant-sulphide model with toxicity delay. More specifically, the effects of discrete delay and distributed delay on the dynamics are explored, respectively. The deep analysis of eigenvalues indicates that both diffusion and delay can induce Hopf bifurcations. The normal form theory is used to set up an exact formula that determines the properties of Hopf bifurcation in a diffusive plant-sulphide model. A sufficiently small discrete delay does not affect the stability and a sufficiently large discrete delay destabilizes the system. Nonetheless, a sufficiently small or large distributed delay does not affect the stability. Both delays cause instability by inducing Hopf bifurcation rather than Turing bifurcation.

1. Introduction

On the intertidal mudflats, plants have the ability to capture suspended particles and make the sediment stable, thus promoting their own growth. Nonetheless, the positive feedback also leads to a negative feedback when organic matter banks up in the sediment. The process of anaerobic decomposition by sulphate-reducing bacteria produces toxic sulphides that, if accumulated in large enough quantities, then cause plant death, see Lamers et al. [15] and Mirlean et al. [20]. Thus, the plant-sulphide feedback framework delineates a mechanism by which sulphide concentrations increase from a process that benefits the plant, but shapes a negative feedback for plant growth.

This paper is committed to studying the spatio-temporal dynamics of the following plant-sulphide model under the Neumann boundary condition,

$$\begin{cases} u_t = D_1\Delta u + \varkappa(Av - \frac{Bk_s u}{k_s+v}), & x\in(0,\ell\pi), t>0,\\ v_t = D_2\Delta v + rv(1-\frac{v}{K}) - Cu(x,t-\tau)v, & x\in(0,\ell\pi), t>0,\\ u_{\mathbf{n}} = v_{\mathbf{n}} = 0, & t\geq 0, x=0,\ell\pi,\\ (u,v)(x,t) = (u_0(x), v_0(x)) \geq 0, & (t,x)\in[-\tau,0]\times[0,\ell\pi]. \end{cases} \tag{1.1}$$

where u and v represent, respectively, sulphide concentration and plant biomass at time t. D_1 and D_2 measure sulphide dispersal and plant lateral expansion, respectively. Δ is the Laplace operator. $\varkappa$ is the control parameter. A denotes the rate at which hydrogen sulphide is produced by plants. B describes the maximal escape rate of hydrogen sulphide. k_s indicates that plants promote the enrichment of sulphides. r and K measure, respectively, reproductive rate and carrying capacity. C describes the plant mortality caused by sulphides.

The biodynamics of ecosystems, including the mechanisms and patterns of spatial dispersal, has become a current focus of mathematical biology. Incorporating diffusion into basic differential equation biological models allows us to more accurately study the lateral expansion of plants and the movement of animals, such as random and density-dependent mobility. A host of scholars have used the reaction-diffusion equation to model and study the biological relationships in various ecosystems. Meanwhile, time lag is another indispensable factor in the modelling process. The addition of diffusion and delay is helpful for us to analyse and understand the real population distribution.

In nature, the species are spatially distributed and interact in diverse spatial location. The biological systems with diffusion have been extensively explored in substantial works. The distinctions among cross-diffusion, self-diffusion and diffusion are expounded by Lou and Ni [18]. Spatial memory with three types of diffusion just mentioned is studied by Shi et al. [22]. Tang and Song [26] studied Turing and Hopf bifurcations of a prey-predator system with self-diffusion and nonlinear mortality. Sun et al. [25] revealed the bistable phenomenon and Turing-Hopf bifurcation in a plant-water system with diffusion. Jiang et al. [12] studied the space-time dynamics of a diffusive Schnakenberg system. Wu and Zhao [31] studied the effects of threshold hunting and Allee effect in a diffusive system. Zhou and Xiao [39] researched a competition-diffusion-advection system. Luo and Wang [19] investigated the pattern dynamics in a reaction-diffusion model with prey-taxis. Lin et al. [17] studied Hopf-Turing bifurcation in reaction-diffusion neural networks. Chen et al. [3] studied the space-time dynamics near a Hopf-Turing bifurcation point of a diffusive model. Yi et al. [35] studied the bifurcations and patterns in a diffusive system, and Wang et al. [28] researched the global bifurcation and patterns of a class of diffusive models. Zhang et al. [36] studied the space-time kinetics in a planktonic model. There are plentiful works on the space-time dynamics of various systems, such as Wu et al. [30], Wu and Hsu [32], Yang et al. [33], Yi et al. [34], Fu et al. [9].

Another important factor in modelling is time delay, which plays a vital role in physics, biology or engineering problems. In biodynamic systems, time delay is generally due to several processes, such as the pregnancy and maturation period, and the lag of the toxic attack. The implications of adding time delays to modelling have been explored by many researchers. Li et al. [16] explored the joint effects of memory and maturation delays by utilizing crossing curves method in a diffusive system. Chen et al. [4] studied Hopf bifurcation of a delayed reaction-diffusion-advection system. Wang and Zou [29] studied the impact of digestion delay on a prey-predator system. Wang et al. [27] analysed the role of maturation delay in prey-predator cycles. Wu and Song [23] investigated the steady state-Hopf bifurcation derived by distributed effect and delay in a diffusive system. There's still lots of research on discrete delay, such as An et al. [1], Zhang et al. [37], Beretta and Breda [2], Kumar and Dubey [13], Everett et al. [8], Kundu and Maitra [14], Dai and Sun [7], Jiang et al. [11].

The dynamics of the various ecosystems mentioned above have been studied to a greater or lesser extent. However, the spatial dynamics of plant patterns in salt marsh systems have seldom been studied. Zhao et al. [38] proposed the following plant-sulphide model in salt marsh ecosystems,

$$\begin{cases} u_t = D_1 \Delta u + \varkappa \left(Av - \frac{Bk_s u}{k_s + v} \right), \\ v_t = D_2 \Delta v + rv \left(1 - \frac{v}{K} \right) - Cuv, \end{cases} \tag{1.2}$$

They found that the occurrence of transient patterns could recognize the ecological courses behind pattern formation and the factors that decide the ecological restoring force. However, their research focuses on modelling and numerical simulations rather than rigorous mathematical analysis. It's pointed out that the toxicity of sulphides does not have an immediate effect on plants, thereby creating a toxicity lag. Therefore, we take into account time lag τ of sulphide toxicity based on their model and study model (1.1). For model (1.1), rescaling

$$\hat{u} = \frac{C}{\sqrt{ACK\eta}} u,\ \hat{v} = \frac{1}{K} v,\ \hat{t} = \sqrt{ACK\eta}\, t,\ a = \frac{r}{\sqrt{ACK\eta}},\ p = \frac{\eta B k_s}{K\sqrt{ACK\eta}},\ q = \frac{k_s}{K},$$
$$d_1 = \frac{D_1}{\sqrt{ACK\eta}},\ d_2 = \frac{D_2}{\sqrt{ACK\eta}},$$

https://doi.org/10.1017/S095679252400069X Published online by Cambridge University Press

removing the hats, then we get the following model with the same boundary condition as model (1.1).

$$\begin{cases} u_t = d_1 \Delta u + v - \frac{qu}{p+v}, \\ v_t = d_2 \Delta v + av(1-v) - u(x, t-\tau)v. \end{cases} \tag{1.3}$$

In addition, the effect of distributed delay on the dynamic behaviour is also important and has captured the attention of numerous scholars. In particular, distributed delay with weak kernel carries profound implications for the study of biodiffusion, e.g. see Cooke and Grossman [6], Gourley and Ruan [10], Shen et al. [21]. Cooke and Grossman [6] showed that it's inherently more stable than discrete delay. The model with distributed toxicity delay is as follows:

$$\begin{cases} u_t = d_1 \Delta u + v - \frac{qu}{p+v}, \\ v_t = d_2 \Delta v + av(1-v) - v \int_{-\infty}^{t} G(t-\eta) u(x, \eta) d\eta, \\ (u, v)(x, t) = (u_0(x), v_0(x)) \geq 0, \ (t, x) \in [-\sigma, 0] \times [0, \ell\pi]. \end{cases} \tag{1.4}$$

where $G(t) = \frac{1}{\sigma} e^{-\frac{t}{\sigma}}$ and other conditions are consistent with system (1.3).

This paper aims to explore the spatio-temporal dynamics of model (1.3) and (1.4) and compare the effects of the discrete delay and distributed delay on model (1.2). One can see our final summary for a detailed comparison.

The structure of remaining paper is as follows. The stability and bifurcation of the local system are explored in Section 2. The stability and the normal form of spatially Hopf bifurcation for the space-time system are computed detailedly in Section 3. The impact of the distributed delay is analysed in Section 4. Numerical illustrations and conclusions are displayed in Section 5 and 6, respectively.

2. Dynamics of the local plant-sulphide model

The local system of (1.3) reads:

$$\begin{cases} \frac{\mathrm{d}u}{\mathrm{d}t} = v - \frac{qu}{p+v}, \\ \frac{\mathrm{d}v}{\mathrm{d}t} = av(1-v) - u(t-\tau)v. \end{cases} \tag{2.1}$$

First, we present several results on system (2.1).

Theorem 2.1. *The solution of system* (2.1) *initiating in* $C([-\tau, 0], \mathbb{R}^2_+)$ *is positive.*

Proof. Let $(u(t), v(t))$ be any solution of system (2.1) with $\tau = 0$. According to $\frac{\mathrm{d}v}{\mathrm{d}t} = av(1-v) - u(t-\tau)v$, we obtain $v(t) = u(0)e^{\int_0^t (a(1-v) - u(t-\tau))dt} > 0$ due to $v(0) > 0$. Accordingly, we get

$$\frac{\mathrm{d}u}{\mathrm{d}t} = v - \frac{qu}{p+v} \geq -\frac{qu}{p+v}.$$

This combined with $u(0) > 0$ shows $u = u(0)e^{-\int_0^t \frac{q}{p+v} dt} > 0$.

By computation, there are two equilibria for system (2.1), namely $E_0(0, 0)$ and $E_*(u_*, v_*)$, where

$$v_* = a(1 - v_*), \ \ v_* = \frac{-(p + aq) + \sqrt{(p + aq)^2 + 4aq}}{2}.$$

Theorem 2.2. *System* (2.1) *possesses two equilibria* $E_0(0, 0)$ *and* $E_*(u_*, v_*)$. *For* $\tau = 0$, E_0 *is a saddle and* E_* *is a stable node or focus.*

Proof. For $\tau = 0$, the Jacobian matrix reads

$$J(u, v) = \begin{pmatrix} -\frac{q}{p+v} & 1 + \frac{qu}{(p+v)^2} \\ -v & a(1-2v) - u \end{pmatrix}. \tag{2.2}$$

https://doi.org/10.1017/S095679252400069X Published online by Cambridge University Press

Hence, we have

$$J(E_0)=\begin{pmatrix} -\frac{q}{p} & 1 \\ 0 & a \end{pmatrix} \text{ and } J(E_*)=\begin{pmatrix} -\frac{q}{p+v_*} & 1+\frac{qu_*}{(p+v_*)^2} \\ -v_* & -av_* \end{pmatrix}.$$

Clearly, E_0 is a saddle. $\mathrm{Tr}(J(E_*))=-av_*-\frac{q}{p+v_*}<0$ and $\det(J(E_*))=\frac{aqv_*}{p+v_*}+(1+\frac{qu_*}{(p+v_*)^2})v_*>0$ indicate that E_* is a stable node or focus.

Theorem 2.3. *For $\tau=0$, there is no limit cycle of system (2.1).*

Proof. Setting $\Theta_1(u,v)=v-\frac{qu}{p+v}$, $\Theta_2(u,v)=av(1-v)-uv$ and choosing the Dulac function $\mathcal{B}(u,v)=\frac{1}{v}$, then we gain

$$\frac{\partial(\Theta_1\mathcal{B})}{\partial u}+\frac{\partial(\Theta_2\mathcal{B})}{\partial v}=-a-\frac{q}{v(p+v)}<0.$$

Thus, no limit cycle emerges in system (2.1) for $\tau=0$.

Theorem 2.4. *For $\tau=0$, if $qu_*^2\le 4ap(p+v_*)^2$, then E_* is globally asymptotic stable for system (2.1) in the interior of the first quadrant.*

Proof. Choose the Lyapunov function

$$\mathcal{V}(u,v)=\int_{u_*}^{u}\frac{\zeta-u_*}{l}d\zeta+\int_{v_*}^{v}\frac{\zeta-v_*}{\zeta}d\zeta$$

for $u,v>0$ and undetermined $l>0$. Then we obtain

$$\begin{aligned}\frac{\mathrm{d}\mathcal{V}}{\mathrm{d}t}&=\frac{1}{l}(u-u_*)\left(v-v_*+\frac{qu_*}{p+v_*}-\frac{qu}{p+v}\right)+(v-v_*)(av_*+u_*-av-u)\\&=\frac{1}{l}\left(u-u_*)(v-v_*+\frac{q(p+v_*)(u_*-u)+qu_*(v-v_*)}{(p+v_*)(p+v)}\right)+(v-v_*)(a(v_*-v)+(u_*-u))\\&=-\frac{q}{l(p+v)}(u-u_*)^2-a(v-v_*)^2+\left(\frac{qu_*}{l(p+v)(p+v_*)}+\frac{1}{l}-1\right)(u-u_*)(v-v_*).\end{aligned}$$

Taking $l=1$ yields

$$\frac{\mathrm{d}\mathcal{V}}{\mathrm{d}t}=-\frac{q}{(p+v)}(u-u_*)^2-a(v-v_*)^2+\left(\frac{qu_*}{(p+v)(p+v_*)}\right)(u-u_*)(v-v_*).$$

Then, we conclude $\frac{qu_*^2}{(p+v)(p+v_*)^2}<4a$ due to $qu_*^2\le 4ap(p+v_*)^2$, namely

$$\left(\frac{qu_*}{(p+v)(p+v_*)}\right)^2<\frac{4aq}{p+v},$$

which implies $\frac{\mathrm{d}\mathcal{V}}{\mathrm{d}t}<0$. This combined with Lasalle invariance principle gains the global asymptotic stability of E_*.

In next section, we're going to show that (2.1) undergoes Hopf bifurcation with certain conditions. The case is covered by Theorem 3.3, thus see Theorem 3.3 for a detailed proof.

3. Dynamics of the spatial plant-sulphide model with discrete delay

Here we take into account delay-driven instability for system (1.3). Linearizing (1.3) at $E_*(u_*,v_*)$ generates

$$\begin{pmatrix} u_t \\ v_t \end{pmatrix}=J_1\begin{pmatrix} \Delta u \\ \Delta v \end{pmatrix}+J_2\begin{pmatrix} u(x,t-\tau) \\ v(x,t-\tau) \end{pmatrix}+J_3\begin{pmatrix} u \\ v \end{pmatrix}, \tag{3.1}$$

https://doi.org/10.1017/S095679252400069X Published online by Cambridge University Press

where

$$J_1=\begin{pmatrix} d_1 & 0\\ 0 & d_2\end{pmatrix},\ J_2=\begin{pmatrix} 0 & 0\\ r_{21} & 0\end{pmatrix},\ J_3=\begin{pmatrix} r_{11} & r_{12}\\ 0 & r_{22}\end{pmatrix}, \tag{3.2}$$

with $r_{11}=-\frac{q}{p+v_*},\ r_{12}=1+\frac{qu_*}{(p+v_*)^2},\ r_{21}=-v_*,\ r_{22}=-av_*$.

Denoting the eigenvalues of

$$\Delta\varepsilon(x)+\theta\varepsilon(x)=0,\ x\in(0,\ell\pi),\ \varepsilon_x|_{x=0,\ell\pi}=0, \tag{3.3}$$

by θ_n, then the corresponding eigenfunctions of $\theta_n=\frac{n^2}{\ell^2}$ are $\varepsilon_n(x)=\cos\frac{n}{\ell}x$.

Setting

$$\begin{pmatrix} u(t,x)\\ v(t,x)\end{pmatrix}=\sum_{n=0}^{\infty}\begin{pmatrix}\mathcal{P}_n\\ \mathcal{Q}_n\end{pmatrix}e^{\lambda_n t}\varepsilon_n(x) \tag{3.4}$$

and plugging it into (3.1) produces the characteristic equation $\Gamma(\lambda)$:

$$\lambda^2-(r_{11}+r_{22}-(d_1+d_2)\theta_n)\lambda+d_1d_2\theta_n^2-(d_1r_{22}+d_2r_{11})\theta_n+r_{11}r_{22}-r_{12}r_{21}e^{-\lambda\tau}=0. \tag{3.5}$$

Then, we see that $\Gamma(0)=d_1d_2\theta_n^2-(d_1r_{22}+d_2r_{11})\theta_n+r_{11}r_{22}-r_{12}r_{21}>0$. As a consequence, E_* is always stable for (1.3) with $\tau=0$, and (1.3) does not undergo Turing bifurcation for $\tau\geq 0$. Therefore, the instability could only be caused by Hopf bifurcation.

For the emergence of Hopf bifurcation, we set iw ($w>0$) a root of (3.5). Plugging it into (3.5) results in

$$\begin{cases}-w^2+d_1d_2\theta_n^2-(d_1r_{22}+d_2r_{11})\theta_n+r_{11}r_{22}-r_{12}r_{21}\cos(w\tau)=0,\\ (r_{11}+r_{22}-(d_1+d_2)\theta_n)w-r_{12}r_{21}\sin(w\tau)=0,\end{cases} \tag{3.6}$$

which leads to

$$w^4+A_nw^2+B_n=0, \tag{3.7}$$

where

$$A_n=(d_1\theta_n-r_{11})^2+(d_2\theta_n-r_{22})^2>0, \tag{3.8}$$

$$B_n=C_nD_n, \tag{3.9}$$

with

$$C_n=d_1d_2\theta_n^2-(d_1r_{22}+d_2r_{11})\theta_n+r_{11}r_{22}+r_{12}r_{21}, \tag{3.10}$$

$$D_n=d_1d_2\theta_n^2-(d_1r_{22}+d_2r_{11})\theta_n+r_{11}r_{22}-r_{12}r_{21}>0. \tag{3.11}$$

If $r_{11}r_{22}+r_{12}r_{21}\geq 0$, then $B_n>0$, which intimates that Eq. (3.7) has no positive root. We thereby consider the positive root Eq. (3.7) under the condition $r_{11}r_{22}+r_{12}r_{21}<0$.

Defining

$$d_2^{(n)}=\frac{d_1r_{22}\theta_n-(r_{11}r_{22}+r_{12}r_{21})}{d_1\theta_n^2-r_{11}\theta_n}, \tag{3.12}$$

then

$$B_n=C_nD_n\begin{cases}>0, & \text{for } d_2>d_2^{(n)},\\ =0, & \text{for } d_2=d_2^{(n)},\\ <0, & \text{for } d_2<d_2^{(n)}.\end{cases} \tag{3.13}$$

Hence, Eq. (3.7) has no positive root for $d_2\geq d_2^{(n)}$ and has a positive root $w^{(n)}$ for $d_2<d_2^{(n)}$, where

$$w^{(n)}=\sqrt{\frac{-A_n+\sqrt{A_n^2-4B_n}}{2}}. \tag{3.14}$$

https://doi.org/10.1017/S095679252400069X Published online by Cambridge University Press

By (3.12), we get

$$d_2^{(n)} \begin{cases} \leq 0, & \text{for } \theta_n \geq \frac{r_{11}r_{22}+r_{12}r_{21}}{d_1 r_{22}}, \\ > 0, & \text{for } \theta_n < \frac{r_{11}r_{22}+r_{12}r_{21}}{d_1 r_{22}}, \end{cases} \tag{3.15}$$

which intimates that Eq. (3.7) has no positive root for $\theta_n \geq \frac{r_{11}r_{22}+r_{12}r_{21}}{d_1 r_{22}}$ and it's possible that Eq. (3.7) has a positive root for $\theta_n < \frac{r_{11}r_{22}+r_{12}r_{21}}{d_1 r_{22}}$.

We first present some results about the root of Eq. (3.7). Let

$$d_2^* = \frac{\ell^2(d_1 r_{22} - (r_{11}r_{22} + r_{12}r_{21})\ell^2)}{d_1 - r_{11}\ell^2}. \tag{3.16}$$

Lemma 3.1. *For Eq. (3.7), we have:*

(A) If $r_{11}r_{22} + r_{12}r_{21} \geq 0$, then there is no positive root for Eq. (3.7);

(B) If $r_{11}r_{22} + r_{12}r_{21} < 0$, then

(I) if $\frac{1}{\ell^2} \geq \frac{r_{11}r_{22}+r_{12}r_{21}}{d_1 r_{22}}$, then there is no positive root for Eq. (3.7).

(II) if $\frac{1}{\ell^2} < \frac{r_{11}r_{22}+r_{12}r_{21}}{d_1 r_{22}}$, then

(i) if $d_2 \geq d_2^*$, then there is no positive root for Eq. (3.7);

(ii) if $d_2 < d_2^*$, then Eq. (3.7) has a positive root.

Proof. For $\frac{1}{\ell^2} \geq \frac{r_{11}r_{22}+r_{12}r_{21}}{d_1 r_{22}}$, we see that $d_2 > 0 \geq d_2^{(n)}$, which means that there is no positive root for Eq. (3.7).

Next we concern ourself with the case: $\frac{1}{\ell^2} < \frac{r_{11}r_{22}+r_{12}r_{21}}{d_1 r_{22}}$. Let

$$f(x) = \frac{d_1 r_{22}x - (r_{11}r_{22} + r_{12}r_{21})}{d_1 x^2 - r_{11}x}, \quad \frac{1}{\ell^2} \leq x < \frac{r_{11}r_{22} + r_{12}r_{21}}{d_1 r_{22}}, \tag{3.17}$$

then

$$f'(x) = \frac{-r_{22}d_{11}^2 x^2 + 2d_1(r_{11}r_{22} + r_{12}r_{21})x - r_{11}(r_{11}r_{22} + r_{12}r_{21})}{(d_1 x - r_{11})^2 x^2}, \tag{3.18}$$

this combined with $r_{11}(r_{11}r_{22} + r_{12}r_{21}) > 0$ shows that $f(x)$ decreases monotonically with respect to x in $[\frac{1}{\ell^2}, \frac{r_{11}r_{22}+r_{12}r_{21}}{d_1 r_{22}})$. Thus, $f(x)$ reaches its maximum value at $x = \frac{1}{\ell^2}$, namely

$$f(x)_{\max} = f(\frac{1}{\ell^2}) = \frac{\ell^2(d_1 r_{22} - (r_{11}r_{22} + r_{12}r_{21})\ell^2)}{d_1 - r_{11}\ell^2} = d_2^*. \tag{3.19}$$

As a result of this, Eq. (3.7) has no positive root for $d_2 \geq d_2^*$ and has a positive root for $d_2 < d_2^*$.

According to $\sin(w\tau) = \frac{(r_{11}+r_{22}-(d_1+d_2)\theta_n)w}{r_{12}r_{21}} > 0$, we obtain

$$\tau^{(n,j)} = \frac{1}{w^{(n)}} \left\{ \arccos\left(\frac{-(w^{(n)})^2 + d_1 d_2 \theta_n^2 - (d_1 r_{22} + d_2 r_{11})\theta_n + r_{11}r_{22}}{r_{12}r_{21}} \right) + 2j\pi \right\}, \tag{3.20}$$

and $j \in \mathbb{N} = \{0, 1, 2, \cdots\}$.

Then we point out that $\tau^{(n,j)}$ increases monotonically with respect to d_2 because of

$$\frac{\mathrm{d}\tau^{(n,j)}}{\mathrm{d}d_2} = \frac{r_{11}\theta_n - d_1\theta_n^2}{r_{12}r_{21}w^{(n)}\sqrt{1-\chi^2}} > 0, \tag{3.21}$$

where

$$\chi = \frac{-(w^{(n)})^2 + d_1 d_2 \theta_n^2 - (d_1 r_{22} + d_2 r_{11})\theta_n + r_{11}r_{22}}{r_{12}r_{21}}.$$

https://doi.org/10.1017/S095679252400069X Published online by Cambridge University Press

Next we verify the transversality condition at $\tau = \tau^{(n,j)}$.

Lemma 3.2. *If $\lambda(\tau) = \beta(\tau) + i\gamma(\tau)$ is a pair of roots of Eq. (3.5) near $\tau = \tau^{(n,j)}$ satisfying $\beta(\tau^{(n,j)}) = 0$ and $\gamma(\tau^{(n,j)}) = w^{(n)}$, then we get $\frac{dRe(\lambda(\tau))}{d\tau}\big|_{\tau=\tau^{(n,j)}} > 0$.*

Proof. Taking the derivative of both sides of Eq. (3.5) with respect to τ yields

$$\frac{\mathrm{d}\lambda(\tau)}{\mathrm{d}\tau} = -\frac{r_{12}r_{21}\lambda e^{-\lambda\tau}}{2\lambda + (d_1+d_2)\theta_n - (r_{11}+r_{22}) + r_{12}r_{21}\tau e^{-\lambda\tau}}, \tag{3.22}$$

that is,

$$\left.\frac{\mathrm{d}Re(\lambda(\tau))}{\mathrm{d}\tau}\right|_{\tau=\tau^{(n,j)}} = \frac{2(w^{(n)})^2 + A_n}{a_{12}^2 a_{21}^2} > 0. \tag{3.23}$$

Combining Lemmas 3.1 and 3.2 ultimately leads to the following statement.

Theorem 3.3. *For system (1.3), we suppose that d_2^* and $\tau^{(n,j)}$ are defined by (3.19) and (3.20), respectively.*

(I) If $\frac{1}{\ell^2} \geq \frac{r_{11}r_{22}+r_{12}r_{21}}{d_1 r_{22}}$, then E_* is stable for $\tau \geq 0$.

(II) If $\frac{1}{\ell^2} < \frac{r_{11}r_{22}+r_{12}r_{21}}{d_1 r_{22}}$, then

(i) if $d_2 \geq d_2^*$, then E_* is stable for $\tau \geq 0$;

(ii) if $d_2 < d_2^*$, then E_* is stable for $\tau < \tau^*$ and is unstable for $\tau > \tau^*$, where

$$\tau^* = \min_{n=0,1,2,\cdots,n_*} \tau^{(n,0)} \tag{3.24}$$

with

$$n_* = \min\{\widehat{n},\ \widetilde{n}\},$$

where $\widetilde{n} = \max\{n \in \mathbb{N}^+ = \{1,2,\cdots\} : D_n < 0\}$ and

$$\widehat{n} = \begin{cases} 1, & \text{if } 1 < n^\# < 2, \\ [n^\#], & \text{if } n^\# \text{ is not an integer and } n^\# \geq 2, \\ n^\# - 1, & \text{if } n^\# \text{ is an integer and } n^\# \geq 2, \end{cases} \quad n^\# = \ell\sqrt{\frac{r_{11}r_{22}+r_{12}r_{21}}{d_1 r_{22}}}, \tag{3.25}$$

where $[\cdot]$ represents the integer part function;

(iii) mode-k spatially inhomogeneous Hopf bifurcations emerge at $\tau = \tau^{(k,j)}$, where $k = 0,1,2,\cdots,n_*$.

Remark 3.4. From Theorem 3.3, we conclude that if d_1 or d_2 is large enough, then E_* is always stable for $\tau \geq 0$. However, the discrete delay τ could cause Hopf bifurcation for the appropriate dispersal rate d_2. And large enough delay τ makes E_* unstable.

Next, we utilize the means in Song et al. [24] so as to achieve the normal formal computation of spatially Hopf bifurcations at $\tau = \tau^{(k,j)}$ with $k = 0,1,2,\cdots,n_*$. For generality, we denote these delay thresholds by τ^* so that (3.5) possesses a pair of purely imaginary roots $\pm w^{(n)}$ represented by $\pm w^*$. Setting

$$\beth := \{(u,v) \in (W^{2,2}(0,\ell\pi))^2 : (u_x, v_x)|_{x=0,\ell\pi} = 0\},$$

$\widehat{u}(t,\cdot) = u(\tau t,\cdot) - u_*$, $\widehat{v}(t,\cdot) = v(\tau t,\cdot) - v_*$, $\widehat{Z}(t) = (\widehat{u}(\cdot,t), \widehat{v}(\cdot,t))$ and then removing the hats, (1.3) turns into

$$Z_t = \tau d\Delta Z(t) + L(\tau)(Z_t) + f(Z_t,\tau), \tag{3.26}$$

https://doi.org/10.1017/S095679252400069X Published online by Cambridge University Press

where

$$\begin{cases} L(\tau)(\phi) = \tau \begin{pmatrix} r_{11}\phi_1(0) + r_{12}\phi_2(0) \\ r_{21}\phi_2(-1) + r_{22}\phi_2(-1) \end{pmatrix}, \\ f(\phi, \tau) = \tau \begin{pmatrix} \sum\limits_{m+s\geq 2} \frac{1}{m!s!} f_{ms}^{(1)} \phi_1^m(0)\phi_2^s(0) \\ \sum\limits_{m+s\geq 2} \frac{1}{m!s!} f_{ms}^{(2)} \phi_1^m(-1)\phi_2^s(0) \end{pmatrix}, \end{cases} \tag{3.27}$$

$$\begin{cases} f^{(1)} = v - \frac{qu}{p+v}, \\ f^{(2)} = av(1-v) - vu(t-\tau), \end{cases} \quad \begin{cases} f_{ms}^{(1)} = \frac{\partial^{m+s}}{\partial u^m \partial v^s}(u_*, v_*), \\ f_{ms}^{(2)} = \frac{\partial^{m+s}}{\partial w^m \partial v^s}(u_*, v_*), \end{cases} \tag{3.28}$$

Setting $\tau = \tau^* + \delta, \delta \in \mathbb{R}$, Eq. (3.26) thereby turns into

$$Z_t = \tau^* d\Delta Z(t) + L(\tau^*(Z(t)) + F(Z_t, \delta), \tag{3.29}$$

where $F(\phi, \delta) = \delta d\Delta\phi(0) + L(\delta)(\phi) + f(\phi, \tau^* + \delta)$ for $\phi \in C$. Hence, $\Lambda_0 = \{\mathrm{i}\tau^* w^*, -\mathrm{i}\tau^* w^*\}$ is the set of eigenvalues. The eigenvalues of $\tau^* d\Delta$ on $\beth$ are $\zeta_k^1 = -n^2 d_1 \tau^*$ and $\zeta_k^2 = -n^2 d_2 \tau^*$ with $n \in \mathbb{N}^+$, and the corresponding normalized eigenfunctions $\alpha_n^{(i)}(x)$ reads

$$\alpha_n^{(1)}(x) = \begin{pmatrix} \beta_n(x) \\ 0 \end{pmatrix}, \ \alpha_n^{(2)}(x) = \begin{pmatrix} 0 \\ \beta_n(x) \end{pmatrix}, \ \text{with } \beta_n(x) = \frac{\cos(nx)}{||\cos(nx)||_{2,2}}, \ n \in \mathbb{N}^+. \tag{3.30}$$

Letting $\mathcal{B}_n = \mathrm{span}\{[v(\cdot), \alpha_n^{(i)}(x)]\alpha_n^{(i)}(x) | v \in C\}$ and assuming that $z_t(\rho) \in C([-1, 0], \mathbb{R}^2)$ with

$$z_t^T(\rho) \begin{pmatrix} \alpha_n^{(1)} \\ \alpha_n^{(2)} \end{pmatrix} \in \mathcal{B}_n, \tag{3.31}$$

then we obtain the equivalent ODE on $\mathbb{R}$ reading

$$\dot{z}(t) = \begin{pmatrix} \zeta_n^{(1)} & 0 \\ 0 & \zeta_n^{(2)} \end{pmatrix} z(t) + L(\tau^*) z_t \tag{3.32}$$

whose characteristic equation is (3.5). Define

$$< \psi(s), \phi(\rho) >= \psi(0)\phi(0) - \int_{-1}^{0} \int_{0}^{\rho} \psi(\xi - \rho) d\eta(\rho) \phi(\xi) d\xi, \ \text{for } \psi \in C^*, \ \phi \in C.$$

Then we get

$$\begin{cases} \Phi_n = (Pe^{\mathrm{i}w^*\tau^*\rho}, \overline{P}e^{-\mathrm{i}w^*\tau^*\rho}), \\ \Psi_n = \mathrm{col}(Q^T e^{\mathrm{i}w^*\tau^* s}, \overline{Q}e^{-\mathrm{i}w^*\tau^* s}), \end{cases}$$

with $< \Phi_n, \Psi_n >= I_2$, where

$$P = \begin{pmatrix} P_1 \\ P_2 \end{pmatrix} = \begin{pmatrix} 1 \\ \frac{\mathrm{i}w^* + d_1 n^2 - r_{11}}{r_{12}} \end{pmatrix}, \ Q = \begin{pmatrix} Q_1 \\ Q_2 \end{pmatrix} = \Xi \begin{pmatrix} 1 \\ \frac{\mathrm{i}w^* + d_1 n^2 - r_{11}}{r_{21}} e^{\mathrm{i}w^*\tau^*} \end{pmatrix}, \tag{3.33}$$

with

$$\Xi = \left(1 + \tau^*(\mathrm{i}w^* + d_1 n^2 - r_{11}) + \frac{(\tau^* r_{22} + e^{\mathrm{i}w^*\tau^*})(\mathrm{i}w^* + d_1 n^2 - r_{11})^2}{r_{12} r_{21}}\right)^{-1}.$$

Utilizing the means in Song et al. [24], we get the following normal form

$$\dot{z} = Bz + \begin{pmatrix} A_{n1} z_1 \delta \\ \overline{A}_{n1} z_2 \delta \end{pmatrix} + \begin{pmatrix} A_{n2} z_1^2 z_2 \\ \overline{A}_{n2} z_1 z_2^2 \end{pmatrix} + O(|z|\delta^2 + |z^4|), \tag{3.34}$$

https://doi.org/10.1017/S095679252400069X Published online by Cambridge University Press

where

$$A_{n1} = -n^2(d_1P_1Q_1 + d_2P_2Q_2) + \mathrm{i}w^*Q^TP, \tag{3.35}$$

$$A_{n2} = -\frac{\mathrm{i}}{2w^*\tau^*}\left(r_{n20}r_{n11} - 2|r_{n11}|^2 - \frac{1}{3}|r_{n02}|^2 + \frac{1}{2}(r_{n21} + b_{n21})\right), \tag{3.36}$$

with

$$r_{n20} = \begin{cases} 0, & n \neq 0, \\ \frac{\tau^*}{\sqrt{\pi}}(b_1Q_1 + b_2Q_2), & n = 0, \end{cases} \quad r_{n11} = \begin{cases} 0, & n \neq 0, \\ \frac{\tau^*}{\sqrt{\pi}}(b_3Q_1 + b_4Q_2), & n = 0, \end{cases}$$

$$r_{n02} = \begin{cases} 0, & n \neq 0, \\ \frac{\tau^*}{\sqrt{\pi}}(\overline{b}_1Q_1 + \overline{b}_2Q_2), & n = 0, \end{cases} \quad r_{n21} = \begin{cases} \frac{3\tau^*}{2\pi}b_4, & n \neq 0, \\ \frac{\tau^*}{\pi}b_4, & n = 0, \end{cases}$$

where

$$\begin{aligned} b_1 &= f_{20}^{(1)}P_1^2 + 2f_{11}^{(1)}P_1P_2 + f_{02}^{(1)}P_2^2, \qquad b_2 = f_{20}^{(2)}P_1^2e^{-2\mathrm{i}w^*\tau^*} + 2f_{11}^{(2)}P_1P_2e^{-\mathrm{i}w^*\tau^*}, \\ b_3 &= f_{20}^{(1)}|P_1|^2 + 2f_{11}^{(1)}\mathrm{Re}\{P_1\overline{P}_2\} + f_{02}^{(1)}|P_2|^2, \quad b_4 = f_{20}^{(2)}|P_1|^2 + 2f_{11}^{(2)}\mathrm{Re}\{P_1\overline{P}_2e^{-\mathrm{i}w^*\tau^*}\}, \\ b_5 &= Q_1\left(f_{30}^{(1)}P_1|P_1|^2 + f_{03}^{(1)}P_2|P_2|^2 + f_{21}^{(1)}(P_1^2|\overline{P}_2| + 2|P_1|^2P_2) + f_{12}^{(1)}(|\overline{P}_1|P_2^2 + 2P_1|P_2|^2)\right) \\ &\quad + Q_2\left(f_{30}^{(2)}P_1|P_1|^2e^{-\mathrm{i}w^*\tau^*} + f_{21}^{(2)}(P_1^2|\overline{P}_2|e^{-2\mathrm{i}w^*\tau^*} + 2|P_1|^2P_2)\right). \end{aligned}$$

And

$$b_{n21} = \begin{cases} M_0 + \frac{\sqrt{2}}{2}M_{2n}, & n \neq 0, \\ M_0, & n = 0, \end{cases} \tag{3.37}$$

where for $j = 0, 2n$,

$$M_j = \frac{2\tau^*}{\sqrt{\pi}}Q^T\begin{pmatrix} c_1h_{j11}^{(1)}(0) + c_2h_{j11}^{(2)}(0) + \overline{c}_1h_{j20}^{(1)}(0) + \overline{c}_2h_{j20}^{(2)}(0) \\ c_3h_{j11}^{(1)}(-1) + \overline{c}_3h_{j20}^{(1)}(-1) + c_4h_{j11}^{(2)}(0) + \overline{c}_4h_{j20}^{(2)}(0) \end{pmatrix},$$

with

$$c_1 = f_{20}^{(1)}P_1 + f^{(1)}P_2, \ c_2 = f_{11}^{(1)}P_1 + f_{02}^{(1)}P_2, \ c_3 = f_{20}^{(2)}P_1e^{-\mathrm{i}w^*\tau^*} + f_{11}^{(2)}P_2, \ c_4 = f_{11}^{(2)}P_1e^{-\mathrm{i}w^*\tau^*},$$

and

$$h_{n20}(\rho) = -\frac{1}{\mathrm{i}w^*\tau^*}\left(r_{n20}e^{-\mathrm{i}w^*\tau^*\rho}P + \frac{1}{3}\overline{a}_{n02}e^{-\mathrm{i}w^*\tau^*\rho}\overline{P}\right) + e^{2\mathrm{i}w^*\tau^*\rho}W_{n1},$$

$$h_{n11}(\rho) = \frac{2}{\mathrm{i}w^*\tau^*}\left(r_{n11}e^{-\mathrm{i}w^*\tau^*\rho}P - \overline{a}_{n11}e^{-\mathrm{i}w^*\tau^*\rho}\overline{P}\right) + W_{n2},$$

where

$$W_{n1} = \begin{pmatrix} \frac{c_{nj}(b_1(2\mathrm{i}w^* - r_{22}e^{-2\mathrm{i}w^*\tau^*}) + b_2r_{12})}{(2\mathrm{i}w^* - r_{11})(2\mathrm{i}w^* - r_{22}e^{-2\mathrm{i}w^*\tau^*}) - r_{12}r_{21}e^{-2\mathrm{i}w^*\tau^*}} \\ \frac{c_{nj}(b_1r_{21}e^{-2\mathrm{i}w^*\tau^*} + b_2(2\mathrm{i}w^* - r_{11}))}{(2\mathrm{i}w^* - r_{11})(2\mathrm{i}w^* - r_{22}e^{-2\mathrm{i}w^*\tau^*}) - r_{12}r_{21}e^{-2\mathrm{i}w^*\tau^*}} \end{pmatrix}, \ W_{n2} = \begin{pmatrix} \frac{2c_{nj}(b_4r_{12} - b_3r_{22})}{r_{11}r_{22} - r_{12}r_{21}} \\ \frac{2c_{nj}(b_3r_{21} - b_4r_{11})}{r_{11}r_{22} - r_{12}r_{21}} \end{pmatrix}, \tag{3.38}$$

and

$$c_{nj} = \begin{cases} \frac{1}{\sqrt{\pi}}, & j = 0, \\ \frac{1}{\sqrt{2\pi}}, & j = 2n \neq 0, \\ 0, & \text{otherwise.} \end{cases} \tag{3.39}$$

Using the polar coordinate transformation, (3.34) turns into

$$\begin{cases} \dot{\kappa} = \varsigma_{n1}\delta\kappa + \varsigma_{n2}\kappa^3 + O(\kappa\delta^2 + |(\kappa, \delta)|^4), \\ \dot{\vartheta} = -w^*\tau^* + O(|\delta, \kappa|), \end{cases} \tag{3.40}$$

where $\varsigma_{n1} = \mathrm{Re}A_{n1}$ and $\varsigma_{n2} = \mathrm{Re}A_{n2}$.

https://doi.org/10.1017/S095679252400069X Published online by Cambridge University Press

From Chow and Hale [5], we conclude that Hopf bifurcation remains supercritical for $\varsigma_{n1}\varsigma_{n2} < 0$ and remains subcritical for $\varsigma_{n1}\varsigma_{n2} > 0$; Hopf bifurcation remains stable for $\varsigma_{n1} < 0$ and remains unstable for $\varsigma_{n1} > 0$.

4. Dynamics of the spatial plant-sulphide model with distributed delay

System (1.3) with distributed delay σ reads:

$$\begin{cases} u_t = d_1\Delta u + v - \frac{qu}{p+v}, \\ v_t = d_2\Delta v + av(1-v) - v\int_{-\infty}^{t} G(t-\eta)u(x,\eta)d\eta, \\ (u,v)(x,0) = (u_0(x), v_0(x)) \geq 0,\ (t,x) \in [-\sigma, 0] \times (0, \ell\pi). \end{cases} \tag{4.1}$$

where $G(t) = \frac{1}{\sigma}e^{-\frac{t}{\sigma}}$ and other conditions are coincident with (1.3).

Linearizing system (4.1) at E_* generates

$$\begin{pmatrix} u_t \\ v_t \end{pmatrix} = J_1 \begin{pmatrix} \Delta u \\ \Delta v \end{pmatrix} + J_2 \begin{pmatrix} \widetilde{u} \\ \widetilde{v} \end{pmatrix} + J_3 \begin{pmatrix} u \\ v \end{pmatrix}, \tag{4.2}$$

where $\widetilde{u} = \int_{-\infty}^{t} G(t-\eta)u(x,\eta)d\eta$, $\widetilde{v} = \int_{-\infty}^{t} G(t-\eta)v(x,\eta)d\eta$, J_i $(i = 1, 2, 3)$ are consistent with (3.2).

Plugging

$$\begin{pmatrix} u \\ v \end{pmatrix} = \sum_{n=0}^{\infty} \begin{pmatrix} \mathcal{P}_n \\ \mathcal{Q}_n \end{pmatrix} e^{\lambda_n t}\varepsilon_n(x) \tag{4.3}$$

into (4.1) produces the characteristic equation $\widehat{\Gamma}(\lambda)$:

$$\begin{aligned} &\lambda^2 - (r_{11} + r_{22} - (d_1 + d_2)\theta_n)\lambda + d_1d_2\theta_n^2 - (d_1r_{22} + d_2r_{11})\theta_n + r_{11}r_{22} \\ &- r_{12}r_{21}\int_0^{+\infty} G(\eta)e^{-\lambda\eta}d\eta = 0. \end{aligned} \tag{4.4}$$

Due to $\lim\limits_{\sigma\to 0^+} G(\eta)e^{-\lambda\eta}d\eta = 1$, thus $\widehat{\Gamma}(0) = \Gamma(0) \neq 0$, which suggests that there's no Turing bifurcation. As a result, Eq. (4.4) becomes

$$\sigma\lambda^3 + \widetilde{A}_n\lambda^2 + \widetilde{B}_n\lambda + \widetilde{C}_n = 0, \tag{4.5}$$

where

$$\begin{aligned} \widetilde{A}_n &= \sigma(d_1 + d_2)\theta_n + 1 - \sigma(r_{11} + r_{22}), \\ \widetilde{B}_n &= \sigma(d_1d_2\theta_n^2 - (d_1r_{22} + d_2r_{11})\theta_n + r_{11}r_{22}) - (r_{11} + r_{22} - (d_1 + d_2)\theta_n), \\ \widetilde{C}_n &= d_1d_2\theta_n^2 - (d_1r_{22} + d_2r_{11})\theta_n + r_{11}r_{22} - r_{12}r_{21}. \end{aligned}$$

It's easy to see $\widetilde{A}_n$, $\widetilde{B}_n$, $\widetilde{C}_n > 0$. In line with the Routh-Hurwitz criterion, we arrive at the following consequence.

Lemma 4.1. *For Eq. (4.5), we have:*

(i) The real parts of whole roots are negative iff $\widetilde{A}_n\widetilde{B}_n - \sigma\widetilde{C}_n > 0$.

(ii) A pair of purely imaginary roots $\pm i\sqrt{\frac{\widetilde{B}_n}{\sigma}}$ *exist iff* $\widetilde{A}_n\widetilde{B}_n - \sigma\widetilde{C}_n = 0$.

Direct calculation displays

$$\widetilde{A}_n\widetilde{B}_n - \sigma\widetilde{C}_n = \widetilde{A}_{n1}\sigma^2 + \widetilde{B}_{n1}\sigma + \widetilde{C}_{n1}, \tag{4.6}$$

https://doi.org/10.1017/S095679252400069X Published online by Cambridge University Press

where

$$\widetilde{A}_{n1} = ((d_1+d_2)\theta_n - (r_{11}+r_{22}))\left(d_1d_2\theta_n^2 - (d_1r_{22}+d_2r_{11})\theta_n + r_{11}r_{22}\right),$$
$$\widetilde{B}_{n1} = ((d_1+d_2)\theta_n - (r_{11}+r_{22}))^2 + r_{12}r_{21},$$
$$\widetilde{C}_{n1} = (d_1+d_2)\theta_n - (r_{11}+r_{22}).$$

It's easy to see $\widetilde{A}_{n1},\ \widetilde{C}_{n1} > 0$. Defining

$$\widehat{d}_2^{(n)} = \frac{r_{11}+r_{22}+\sqrt{-r_{12}r_{21}}}{\theta_n} - d_1, \tag{4.7}$$

then $\widetilde{B}_{n1} > 0$ for $d_2 > \widehat{d}_2^{(n)}$. It's not hard to demonstrate that the maximum value of $\widehat{d}_2^{(n)}$ is

$$\max_{n\in\mathbb{N}^+} \widehat{d}_2^{(n)} = (r_{11}+r_{22}+\sqrt{-r_{12}r_{21}})\ell^2 - d_1 \triangleq d_2^{\#}. \tag{4.8}$$

Thereby Eq. (4.6) has no positive roots for $d_2 \geq d_2^{\#}$ and it's possible that Eq. (4.6) possesses positive roots for $d_2 < d_2^{\#}$.

Clearly, the equation $\widetilde{A}_{n1}\sigma^2 + \widetilde{B}_{n2}\sigma + \widetilde{C}_{n1} = 0$ possesses two positive roots σ_n^- and σ_n^+ $(\sigma_n^- < \sigma_n^+)$ iff $\widetilde{B}_{n1}^2 - 4\widetilde{A}_{n1}\widetilde{C}_{n1} > 0,\ \widetilde{B}_{n1} < 0$, where

$$\sigma_n^- = \frac{-\widetilde{B}_{n1} - \sqrt{\widetilde{B}_{n1}^2 - 4\widetilde{A}_{n1}\widetilde{C}_{n1}}}{2\widetilde{A}_{n1}},$$
$$\sigma_n^+ = \frac{-\widetilde{B}_{n1} + \sqrt{\widetilde{B}_{n1}^2 - 4\widetilde{A}_{n1}\widetilde{C}_{n1}}}{2\widetilde{A}_{n1}}.$$

Define

$$S = \{n \in \mathbb{N}^+ : \widetilde{B}_{n1}^2 - 4\widetilde{A}_{n1}\widetilde{C}_{n1} > 0,\ \widetilde{B}_{n1} < 0\},$$

which is obviously a finite set.

The following transversality condition at $\sigma = \sigma_n^{\pm}$ holds.

$$\begin{aligned}\left.\frac{\mathrm{d}Re(\lambda(\sigma))}{\mathrm{d}\sigma}\right|_{\sigma=\sigma_n^{\pm}} &= -\frac{\frac{\mathrm{d}\widetilde{A}_n}{\mathrm{d}d_2}\lambda^2 + \frac{\mathrm{d}\widetilde{B}_n}{\mathrm{d}d_2}\lambda + \frac{\mathrm{d}\widetilde{C}_n}{\mathrm{d}d_2}}{3\sigma_n^{\pm}\lambda^2 + 2\widetilde{A}_n\lambda + \widetilde{B}_n} \\ &= \frac{(\sigma_n^{\pm})^2(d_1\theta_n^2 - r_{11}\theta_n)(r_{11}+r_{22}-(d_1+d_2)\theta_n) - (\sigma\widetilde{B}_n + \widetilde{A}_n)\theta_n}{2(\widetilde{A}_n^2 + \sigma_n^{\pm}\widetilde{B}_n)} \\ &< 0.\end{aligned}$$

This combined with Lemma 4.1 obtains the following consequence.

Theorem 4.2. *For system (4.1), $d_2^{\#}$ is defined by (4.8), then we have:*

(I) If $d_2 \geq d_2^{\#}$, then E_* is stable for $\sigma \geq 0$.

(II) If $d_2 < d_2^{\#}$, then

(i) E_* is stable for $\sigma < \sigma_*$ or $\sigma > \sigma^*$ and is unstable for $\sigma_* < \sigma < \sigma^*$, where

$$\sigma_* = \min_{n\in S}\sigma_n^-,\ \sigma^* = \max_{n\in S}\sigma_n^+;$$

(ii) Hopf bifurcations emerge at $\sigma = \sigma_n^{\pm}$ for $n \in S$.

Remark 4.3. From (4.6) and Theorem 4.2, we conclude that if d_1 or d_2 is large enough, then E_* is always stable for $\sigma \geq 0$. However, the distributed delay σ could cause Hopf bifurcation for the appropriate dispersal rate d_2. In contrast to the discrete delay τ, a sufficiently large distributed delay σ still makes E_* stable. That is, the stability interval for the distributed delay is larger than that for the discrete delay.

https://doi.org/10.1017/S095679252400069X Published online by Cambridge University Press

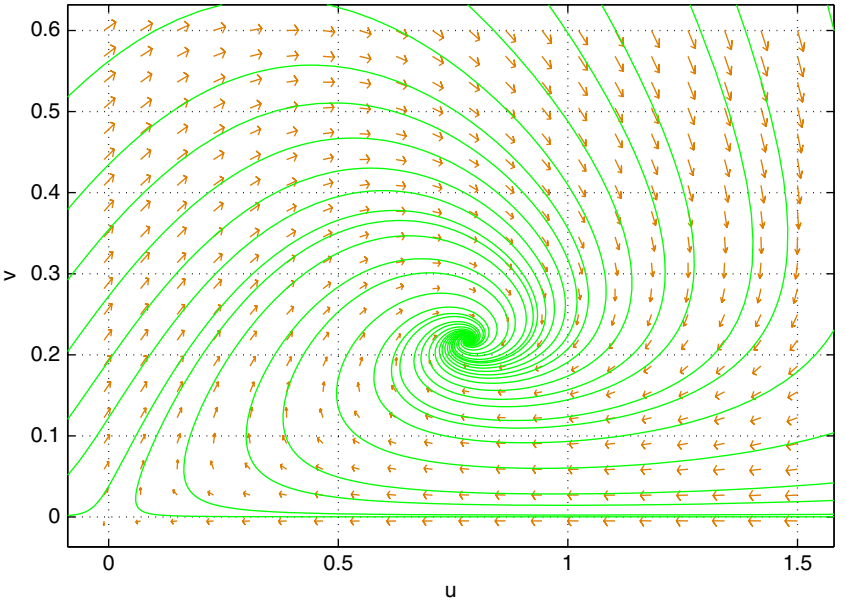

Figure 1. *Taking* $(a, p, q) = (1, 0.5, 0.2)$*, then* $E_*(0.7821, 0.2179)$ *of (2.1) with* $\tau = 0$ *is globally asymptotic stable.*

5. Numerical results

For system (1.3), we fix the parameters $(a, p, q, d_1, \ell) = (1, 0.5, 0.2, 0.02, 1)$ and vary the parameters (τ, d_2) in order to illustrate numerically the results mentioned above.

Figure 1 depicts the global stability of E_* for the non-delay system (2.1). For fixed $d_2 = 0.024$, we get $d_2^* = 0.7333$ and $n_* = \min\{\widehat{n}, \widetilde{n}\} = \min\{7, 3\} = 3$, which intimates that mode-k spatially inhomogeneous Hopf bifurcations emerge at $\tau = \tau^{(k,j)}$, $k = 1, 2, 3$. System (2.1) undergoes spatially homogeneous Hopf bifurcation near $\tau = \tau^{(0,0)}$.

For system (2.1), Figure 2 depicts the stability and Hopf bifurcation near $E_*(0.7821, 0.2179)$. For system (1.3), Figure 3 presents the stability region of the $\tau - d_2$ plane. Figure 4 explains the stability when $d_2 > d_2^* = 0.7333$ and Figure 5 explains the stability when $d_2 < d_2^*$. Figures 6 and 7 reveal, respectively, the periodic solutions arising from spatially homogeneous and mode-3 Hopf bifurcation. Taking $n = 0$ and $n = 3$ for example, we calculate the coefficient to be $\varsigma_{01} = 0.6522$, $\varsigma_{02} = -0.2584$, and $\varsigma_{31} = 0.0977$, $\varsigma_{32} = -0.5661$. This suggests that the spatially homogeneous Hopf bifurcation in Figure 6 and mode-3 Hopf bifurcation in Figure 7 are all supercritical and stable.

For system (1.4), we choose $(a, p, q, d_1, d_2, \ell) = (1, 1, 0.1, 0.01, 0.1, 4)$, then we obtain $E_*(0.9156, 0.0844)$ and $d_2^{\#} = 1.9904 > d_2$. In order to implement numerical simulations of system (4.1), we introduce the equivalent system by setting $w(x, t) = \int_{-\infty}^{t} G(t - \eta)u(x, \eta)d\eta$.

$$\begin{cases} u_t = d_1 \Delta u + v - \frac{qu}{p+v}, \\ v_t = d_2 \Delta v + av(1 - v) - vw, \\ w_t = \frac{1}{\sigma}(u - w). \end{cases} \tag{5.1}$$

Because of the complexity of formulas $\widetilde{B}_{n1}$ and $\Delta_n = \widetilde{B}_{n1}^2 - 4\widetilde{A}_{n1}\widetilde{C}_{n1}$, we determine set $S = \{1, 2\}$ by numerical simulations under the target parameters, see Figure 8. Thus, we have $\sigma_1^- = 3.5390 < \sigma_2^- = 5.38 < \sigma_2^+ = 17.9333 < \sigma_1^+ = 33.5642$, which means $\sigma_* = 3.5390, \sigma^* = 33.5642$. By choosing the values of the gradually increasing σ, we demonstrate the correctness of Theorem 4.2. Figures 9 and 10

https://doi.org/10.1017/S095679252400069X Published online by Cambridge University Press

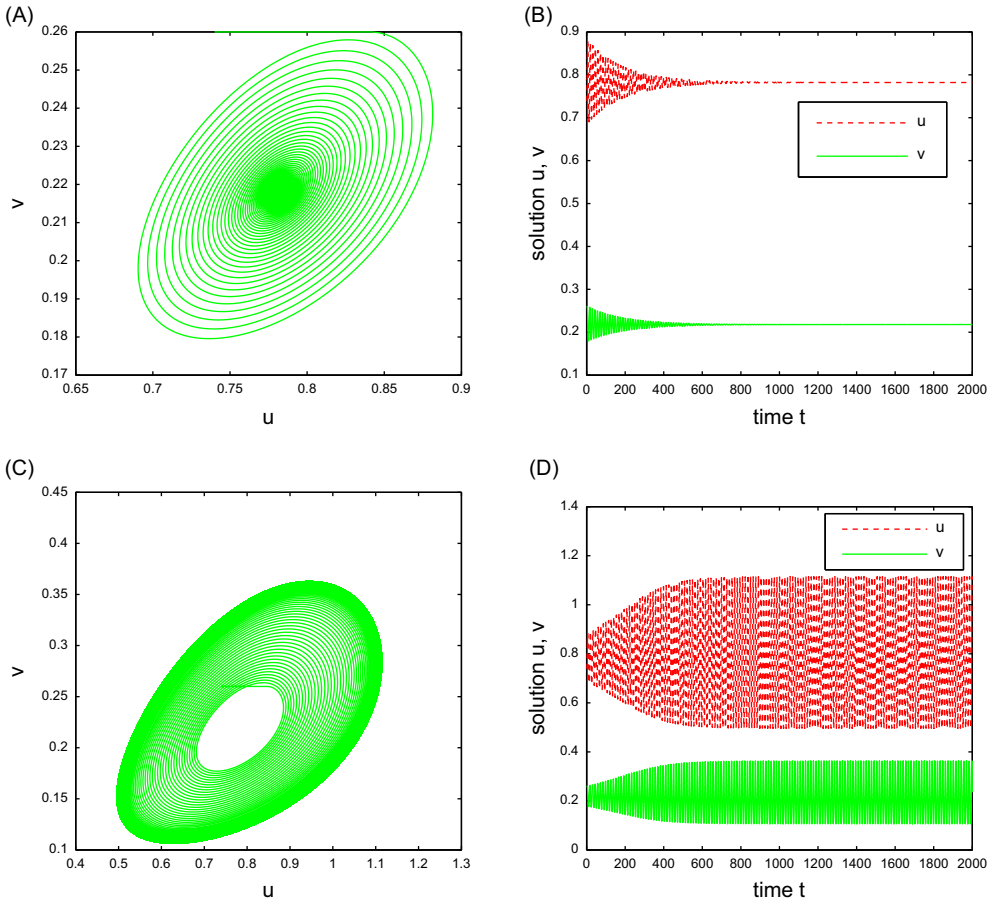

Figure 2. *Taking* $\tau = 1.95 < \tau^{(0,0)} = 2.0537$, *then* (*A*) *and* (*B*) *show that* E_* *is stable. Taking* $\tau = 2.1 > \tau^{(0,0)}$, *then* (*C*) *and* (*D*) *show that a stable limit cycle arises.*

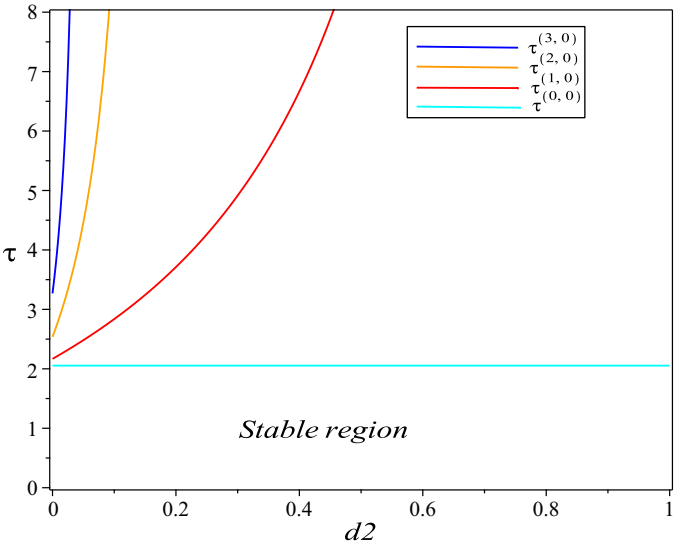

Figure 3. *Stable region in the* $\tau - d_2$ *plane.*

https://doi.org/10.1017/S095679252400069X Published online by Cambridge University Press

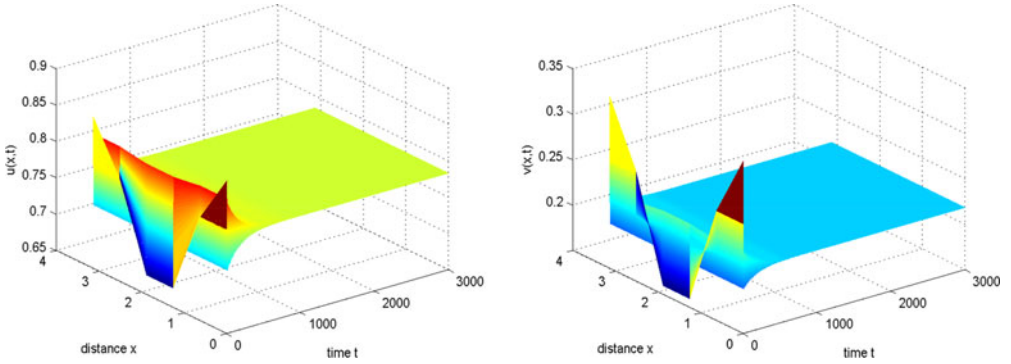

Figure 4. *Taking* $d_2 = 0.78 > d_2^* = 0.7333$, $\tau = 1.95$, *then* E_* *is always stable. The initial conditions are* $u_0(x) = 0.76 + 0.1\cos 2x$ *and* $v_0(x) = 0.24 + 0.1\cos 2x$.

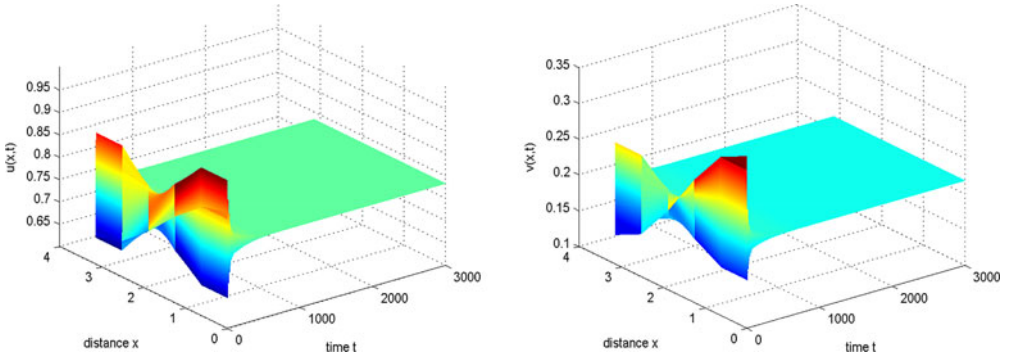

Figure 5. *Taking* $d_2 = 0.024, \tau = 1.95 < \tau^{(0,0)}$, *then* E_* *is stable. The initial conditions are* $u_0(x) = 0.76 + 0.1\cos x$ *and* $v_0(x) = 0.24 + 0.1\cos x$.

depict that E_* is stable. Figure 11 describes a series of inhomogeneous periodic solutions at $\sigma = \sigma_j^{\pm}$ $(j = 1, 2)$. And all initial values are $u_0(x) = w_0(x) = 0.9156 + 0.1\cos x$, $v_0(x) = 0.0844 + 0.01\cos x$.

6. Conclusion

The aim of this paper is to research the impacts of time lag and diffusion on the system. We deliberate different time lag on the space-time system. We analyse the stability and bifurcation in detail and discover that both the discrete delay and distributed delay do not induce Turing bifurcation. Simply put, the instability could only be caused by Hopf bifurcation. We judge the direction and stability of periodic solutions by deducing the normal form. We found that appropriate time lag destabilizes the system, and there is a series of delay thresholds inducing Hopf bifurcations. Our findings once again demonstrate the importance of time lag in biodiffusion. Through Remarks 3.4 and 4.3, the findings are summarized below.

Common grounds:

(i) Neither of these two delays induces Turing bifurcation.

(ii) These two delays τ and σ do not change the stability if sulphides disperse quickly or plants expand laterally quickly. Nonetheless, if sulphides disperse slowly, then delays τ and σ do not alter the

https://doi.org/10.1017/S095679252400069X Published online by Cambridge University Press

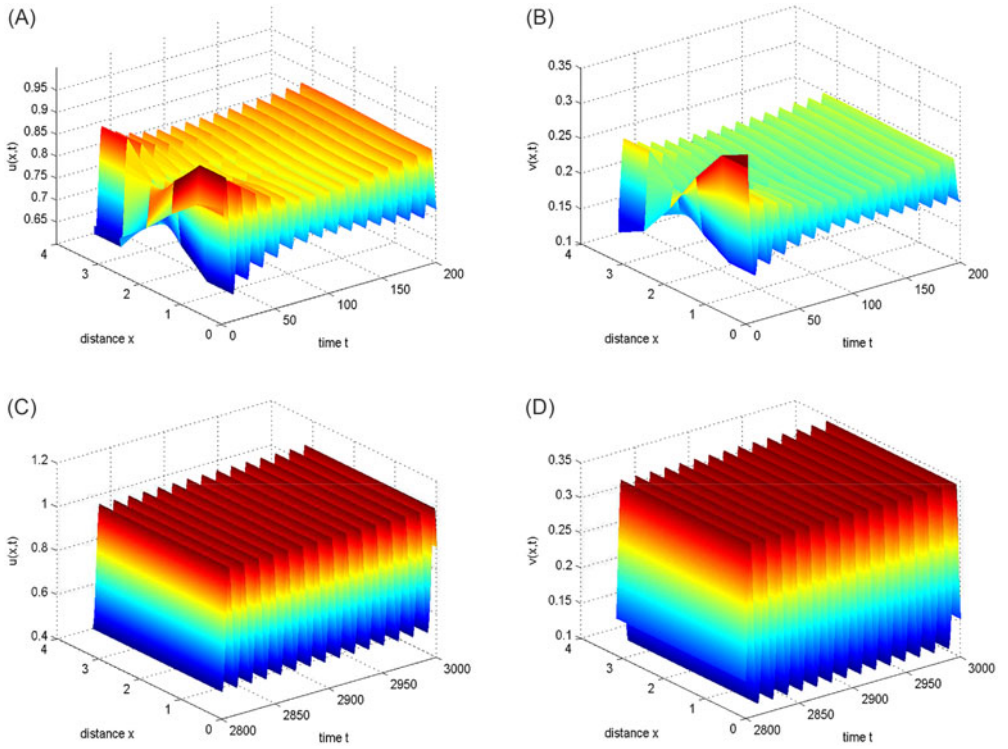

Figure 6. *Taking* $d_2 = 0.024, \tau = 2.1 > \tau^{(0,0)}$*, then stable spatially homogeneous periodic solutions appear. The initial conditions are* $u_0(x) = 0.76 + 0.1\cos x$ *and* $v_0(x) = 0.24 + 0.1\cos x$.

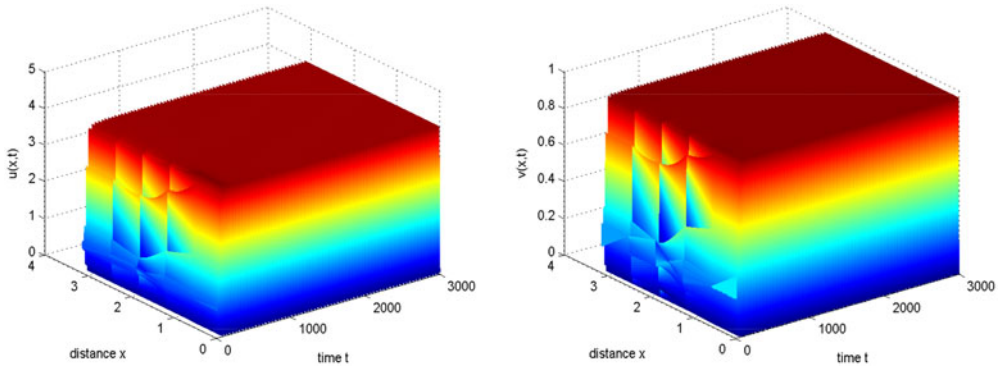

Figure 7. *Taking* $d_2 = 0.024, \tau = 6.98 > \tau^{(3,0)} = 6.8066$*, then stable spatially inhomogeneous periodic solutions arise from mode-3 Hopf bifurcation. The initial conditions are* $u_0(x) = 0.76 + 0.1\cos 3x$ *and* $v_0(x) = 0.24 + 0.1\cos 3x$.

stability as plants expand laterally quickly, and delays τ and σ could induce Hopf bifurcation as plants expand slowly.

Differences:

If plants expand laterally slowly, then the stability interval induced by distributed delay σ is much larger than that of discrete delay τ. More specifically, in the case of the discrete delay and small enough d_2 (the rate of plant lateral expansion), large enough delay τ makes E_* unstable. However, in the case of the distributed delay and small enough d_2, large enough delay σ still makes E_* stable.

https://doi.org/10.1017/S095679252400069X Published online by Cambridge University Press

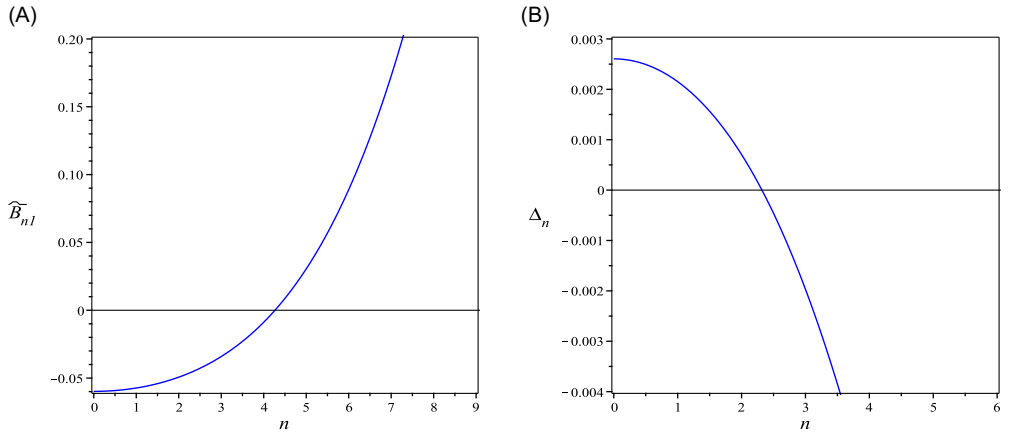

Figure 8. *Taking* $(a, p, q, d_1, d_2, \ell) = (1, 1, 0.1, 0.01, 0.1, 4)$*, then* (A) *and* (B) *denote the graphs of* $\widetilde{B}_{n1}$ *and* $\Delta_n = \widetilde{B}_{n1}^2 - 4\widetilde{A}_{n1}\widetilde{C}_{n1}$*, respectively. Then we obtain* $S = \{1, 2\}$.

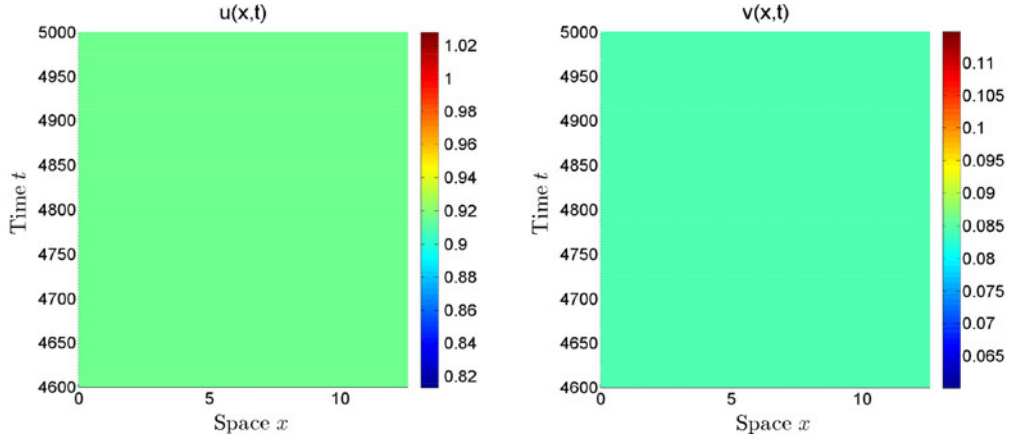

Figure 9. *For fixed* $(a, p, q, d_1, d_2, \ell) = (1, 1, 0.1, 0.01, 0.1, 4)$*, we take* $\sigma = 3.02 < \sigma_* = 3.5390$*, then* E_* *is stable.*

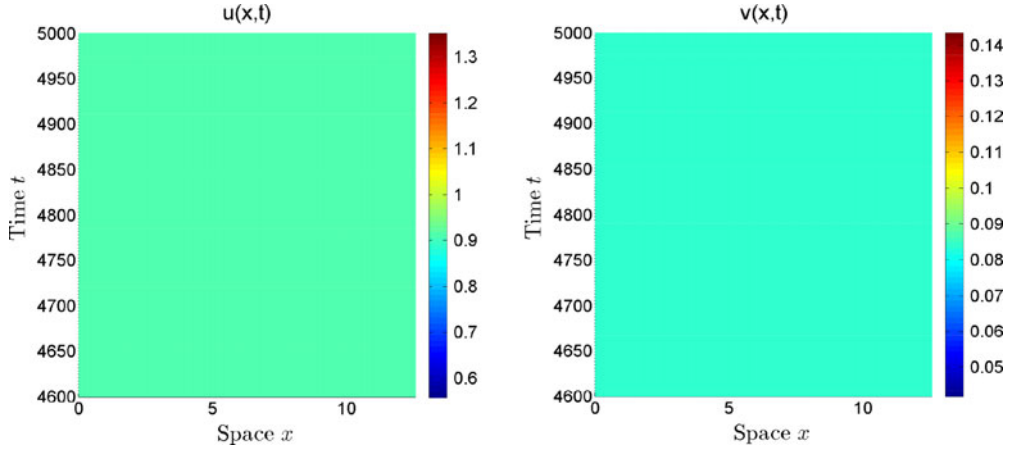

Figure 10. *For fixed* $(a, p, q, d_1, d_2, \ell) = (1, 1, 0.1, 0.01, 0.1, 4)$*, we take* $\sigma = 45 > \sigma^* = 33.5642$*, then* E_* *is stable.*

https://doi.org/10.1017/S095679252400069X Published online by Cambridge University Press

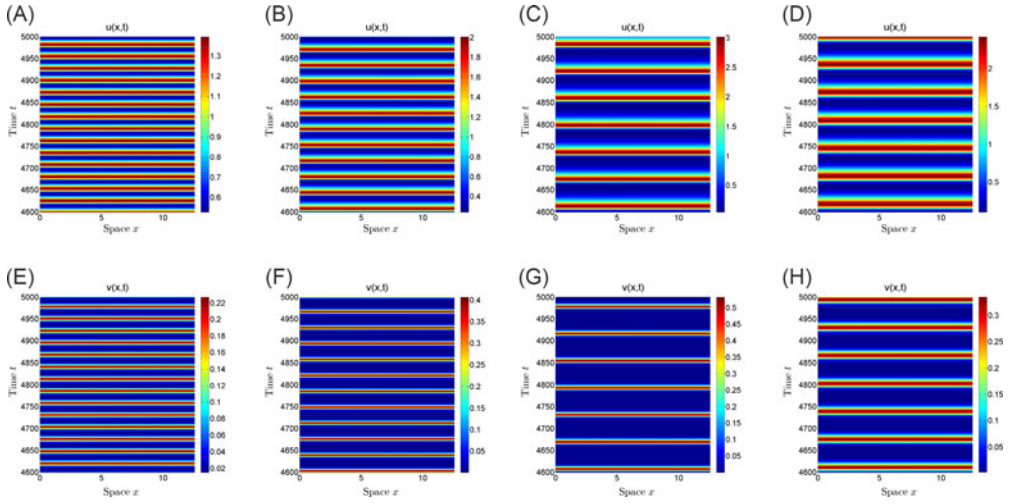

Figure 11. *For fixed* $(a, p, q, d_1, d_2, \ell) = (1, 1, 0.1, 0.01, 0.1, 4)$*, we vary the values of* σ *to get different periodic solutions.* (*a*) *and* (*e*)*:* $\sigma = 3.56 > \sigma_1^- = 3.5390$*.* (*b*) *and* (*f*)*:* $\sigma = 5.42 > \sigma_2^- = 5.38$*.* (*c*) *and* (*g*)*:* $\sigma = 17.6 < \sigma_2^+ = 17.9333$*.* (*e*) *and* (*h*)*:* $\sigma = 33.4 < \sigma_1^+ = 33.5642$*.*

Funding statement. This work was jointly supported by the National Natural Science Foundation of China (No. 12331017 and No. 12071074), and the Zhejiang Provincial Natural Science Foundation of China (No. LZ24A010006).

Competing interests. The authors declare that they have no conflict of interest.

Author contributions. We declare that the authors are ranked in alphabetic order of their names and all of them have the same contributions to this paper.

References

[1] An, Q., Wang, C. & Wang, H. (2020) Analysis of a spatial memory model with nonlocal maturation delay and hostile boundary condition. *Discrete Contin. Dyn. Syst.* **40**, 5845–5868.
[2] Beretta, E. & Breda, D. (2016) Discrete or distributed delay? Effects on stability of population growth. *Math. Biosci. Eng.* **13**(1), 19–41.
[3] Chen, M., Wu, R., Liu, B. & Chen, L. (2019) Spatiotemporal dynamics in a ratio-dependent predator-prey model with time delay near the Turing-Hopf bifurcation point. *Commun. Nonlinear Sci. Numer. Simul.* **77**, 141–167.
[4] Chen, S., Lou, Y. & Wei, J. (2018) Hopf bifurcation in a delayed reaction-diffusion-advection population model. *J. Differ. Equ.* **264**(8), 5333–5359.
[5] Chow, S. & Hale, J. (1982) *Methods of Bifurcation Theory*, Springer, New York.
[6] Cooke, K. & Grossman, Z. (1982) Discrete delay, distributed delay and stability switches. *J. Math. Anal. Appl.* **86**(2), 592–627.
[7] Dai, B. & Sun, G. (2021) Turing-Hopf bifurcation of a delayed diffusive predator-prey system with chemotaxis and fear effect. *Appl. Math. Lett.* **111**, 106644.
[8] Everett, R., Nagy, J. & Kuang, Y. (2016) Dynamics of a data based ovarian cancer growth and treatment model with time delay. *J. Dyn. Differ. Equ.* **28**(3-4), 1393–1414.
[9] Fu, S., He, X., Zhang, L. & Wen, Z. (2021) Turing patterns and spatiotemporal patterns in a tritrophic food chain model with diffusion. *Nonlinear Anal. Real World Appl.* **59**, 103260.
[10] Gourley, S. & Ruan, S. (2000) Dynamics of the diffusive Nicholson's blowflies equation with distributed delay. *Proc. Roy. Soc. Edinburgh Sect. A* **130**(6), 1275–1291.
[11] Jiang, W., An, Q. & Shi, J. (2020) Formulation of the normal form of Turing-Hopf bifurcation in partial functional differential equations. *J. Differ. Equ.* **268**(10), 6067–6102.
[12] Jiang, W., Wang, H. & Cao, X. (2019) Turing instability and Turing-Hopf bifurcation in diffusive Schnakenberg systems with gene expression time delay. *J. Dyn. Differ. Equ.* **31**(4), 2223–2247.
[13] Kumar, A. & Dubey, B. (2019) Modeling the effect of fear in a prey-predator system with prey refuge and gestation delay. *Int. J. Bifurc. Chaos* **29**(14), 1950195.

https://doi.org/10.1017/S095679252400069X Published online by Cambridge University Press

[14] Kundu, S. & Maitra, S. (2018) Dynamical behaviour of a delayed three species predator-prey model with cooperation among the prey species. *Nonlinear Dyn.* **92**(2), 627–643.
[15] Lamers, L., Govers, L., Janssen, I., et al. (2013) Sulfide as a soil phytotoxin-A review. *Front. Plant Sci.* **4**, 00268
[16] Li, S., Yuan, S., Jin, Z. & Wang, H. (2023) Bifurcation analysis in a diffusive predator-prey model with spatial memory of prey, Allee effect and maturation delay of predator. *J. Differ. Equ.* **357**, 32–63.
[17] Lin, J., Xu, R. & Li, L. (2020) Turing-Hopf bifurcation of reaction-diffusion neural networks with leakage delay. *Commun. Nonlinear Sci. Numer. Simul.* **85**, 105241.
[18] Lou, Y. & Ni, W. (1996) Diffusion, self-diffusion and cross-diffusion. *J. Differ. Equ.* **131**(1), 79–131.
[19] Luo, D. & Wang, Q. (2022) Global bifurcation and pattern formation for a reaction-diffusion predator-prey model with prey-taxis and double Beddington-DeAngelis functional responses. *Nonlinear Anal. Real World Appl.* **67**, 103638.
[20] Mirlean, N. & Costa, C. (2017) Geochemical factors promoting die-back gap formation in colonizing patches of Spartina densiflora in an irregularly flooded marsh. *Estuar. Coast. Shelf Sci.* **189**, 104–114.
[21] Shen, H., Song, Y. & Wang, H. (2023) Bifurcations in a diffusive resource-consumer model with distributed memory. *J. Differ. Equ.* **347**, 170–211.
[22] Shi, J., Wang, C. & Wang, H. (2021) Spatial movement with diffusion and memory-based self-diffusion and cross-diffusion. *J. Differ. Equ.* **305**, 242–269.
[23] Wu, S. & Song, Y. (2020) Spatiotemporal dynamics of a diffusive predator-prey model with nonlocal effect and delay. *Commun. Nonlinear Sci. Numer. Simul.* **89**, 105310.
[24] Song, Y., Peng, Y. & Zou, X. (2014) Persistence, stability and Hopf bifurcation in a diffusive ratio-dependent predator-prey model with delay. *Int. J. Bifurc. Chaos* **24**(07), 1450093.
[25] Sun, G., Zhang, H., Song, Y., Li, L. & Jin, Z. (2022) Dynamic analysis of a plant-water model with spatial diffusion. *J. Differ. Equ.* **329**, 395–430.
[26] Tang, X. & Song, Y. (2015) Bifurcation analysis and Turing instability in a diffusive predator-prey model with herd behavior and hyperbolic mortality. *Chaos Solitons Fractals* **81**, 303–314.
[27] Wang, H., Nagy, J., Gilg, O. & Kuang, Y. (2009) The roles of predator maturation delay and functional response in determining the periodicity of predator-prey cycles. *Math. Biosci.* **221**(1), 1–10.
[28] Wang, J., Wei, J. & Shi, J. (2016) Global bifurcation analysis and pattern formation in homogeneous diffusive predator-prey systems. *J. Differ. Equ* **260**(4), 3495–3523.
[29] Wang, Y. & Zou, X. (2020) On a predator-prey system with digestion delay and anti-predation strategy. *J. Nonlinear Sci.* **30**(4), 1579–1605.
[30] Wu, C., Wang, Y. & Zou, X. (2019) Spatial-temporal dynamics of a Lotka-Volterra competition model with nonlocal dispersal under shifting environment. *J. Differ. Equ.* **267**(8), 4890–4921.
[31] Wu, D. & Zhao, H. (2020) Spatiotemporal dynamics of a diffusive predator-prey system with Allee effect and threshold hunting. *J. Nonlinear Sci.* **30**(3), 1015–1054.
[32] Wu, S. & Hsu, C. (2018) Spatial dynamics of multilayer cellular neural networks. *J. Nonlinear Sci.* **28**(1), 3–41.
[33] Yang, Y., Zou, L. & Hsu, C. (2022) Global attractivity of a nonlocal reaction-diffusion viral infection model. *Proc. Am. Math. Soc.* **150**(7), 2901–2911.
[34] Yi, F. (2021) Turing instability of the periodic solutions for reaction-diffusion systems with cross-diffusion and the patch model with cross-diffusion-like coupling. *J. Differ. Equ.* **281**, 379–410.
[35] Yi, F., Wei, J. & Shi, J. (2009) Bifurcation and spatiotemporal patterns in a homogeneous diffusive predator-prey system. *J. Differ. Equ.* **246**(5), 1944–1977.
[36] Zhang, T., Liu, X., Meng, X. & Zhang, T. (2018) Spatio-temporal dynamics near the steady state of a planktonic system. *Comput. Math. Appl.* **75**(12), 4490–4504.
[37] Zhang, Y., Xie, L., Dong, Y., Huang, J., Ruan, S. & Takeuchi, Y. (2023) Bifurcation analysis in a tumor-immune system interaction model with dendritic cell therapy and immune response delay. *SIAM J. Appl. Math.* **83**(5), 1892–1914.
[38] Zhao, L., Zhang, K., Siteur, K., Li, X., Liu, Q. & Koppel, J. (2021) Fairy circles reveal the resilience of self-organized salt marshes. *Sci. Adv.* **7**, 1–12
[39] Zhou, P. & Xiao, D. (2018) Global dynamics of a classical Lotka-Volterra competition-diffusion-advection system. *J. Funct. Anal.* **275**(2), 356–380.

Cite this article: Xia Y., Xiao J. and Yu J. (2025). A diffusive plant-sulphide model: spatio-temporal dynamics contrast between discrete and distributed delay. *European Journal of Applied Mathematics*, **36**, 811–828. https://doi.org/10.1017/S095679252400069X